

## Original Article

## A “seed”-based molecular networking strategy for the screening and identification of unknown glucocorticoids in cosmetics

Dong Guo<sup>a</sup>, Yaxiong Liu<sup>a</sup>, Jingwen Liang<sup>a</sup>, Yayang Huang<sup>b</sup>, Yangjie Li<sup>a</sup>, Qunyue Wu<sup>a</sup>, Sheng Yin<sup>c</sup>, Jihui Fang<sup>a,\*</sup><sup>a</sup>Cosmetics Department, Guangdong Institute for Drug Control, Guangzhou, 510006, China<sup>b</sup>School of Pharmaceutical Sciences, Guangzhou Medical University, Guangzhou, 510006, China<sup>c</sup>School of Pharmaceutical Sciences, Sun Yat-sen University, Guangzhou, 510006, China

## ARTICLE INFO

## Keywords:

Glucocorticoids

In silico

Non-targeted screening

Molecular networking

## ABSTRACT

The illegal addition of glucocorticoids in cosmetics has become a growing concern. However, due to the covert use of these additives, traditional targeted analytical methods have proven inadequate in addressing the evolving regulatory landscape. To tackle this issue, our study employed a “seed”-based molecular networking strategy for the non-targeted detection of glucocorticoids in cosmetics obtained through market surveillance. By utilizing 36 known glucocorticoids as “seed” nodes, we successfully constructed visualized molecular networking spectra for seven cosmetic products. Then, leveraging the data mining capabilities of MS-DIAL and MS-FINDER, 14 potentially risk substances were successfully identified, including newly discovered glucocorticoids, such as dexamethasone phosphate (Dex-P), prednylidene, and 7 alpha-thiospironolactone. To ensure the reliability of our findings, we proposed fragmentation pathways for the newly discovered glucocorticoids. Subsequent analyses involving molecular docking and molecular dynamics simulations indicated that these newly identified glucocorticoids could trigger skin atrophy and endocrine disorders, with Dex-P having the potential to exhibit the most potent impact. Furthermore, the accuracy of the Dex-P identification was validated through standard reference analysis, and its presence was confirmed in additional actual samples. This study presents an efficient methodology for regulating glucocorticoids in cosmetics and provides new insights into the scientific supervision of cosmetics.

## 1. Introduction

Glucocorticoids, a class of steroid hormones, are widely prescribed for treating conditions, such as inflammation, allergies, and autoimmune diseases [1,2]. Nevertheless, increasing research has indicated that long-term or high-dose use of glucocorticoids can lead to a range of adverse effects, including type 2 diabetes, osteoporosis, and skin atrophy [3,4]. Furthermore, certain glucocorticoids have been associated with potential carcinogenicity, endocrine disruption, and developmental abnormalities [5-7]. Despite these risks, some cosmetic manufacturers illegally add glucocorticoids for short-term effects to achieve whitening and acne removal effects [8,9]. Consequently, the use of glucocorticoids in cosmetics is strictly regulated and has become a focal point of cosmetic safety monitoring.

Currently, the detection of glucocorticoids in cosmetics primarily relies on targeted screening using reference standards [9-11]. For instance, Jian *et al.* employed a Ultra-Performance liquid chromatography - tandem mass spectrometry (UPLC-MS/MS) method with precursor ion scanning to analyze 60 samples, identifying seven glucocorticoids in six samples [10]. Similarly, Kim *et al.* developed an LC-MS/MS method capable of simultaneously detecting 43 glucocorticoids in cosmetics, discovering that approximately 25.3% of 95 cosmetic samples contained these compounds [11]. However,

unscrupulous manufacturers may employ covert methods to illegally add glucocorticoids, complicating the effectiveness of standard-based targeted screening in meeting regulatory requirements [12-14]. Huang *et al.* utilized a self-built high-resolution mass spectrometry (MS) library to screen cosmetic samples, identifying methylprednisolone in two batches of whitening cosmetics during the qualitative analysis of unknown substances [12]. In another study, a researcher inferred a new suspected glucocorticoid compound to be betamethasone butyrate acetate [13]. Yang *et al.* detected a suspected glucocorticoid with the same mass spectrum fragments as betamethasone acetate in cosmetics and confirmed it as clobetasol acetate using high-resolution MS [14]. While the frequency of hormone additions to cosmetics has decreased, hormones remained the primary illegal additive in these products [8]. Therefore, utilizing the non-targeted screening method to systematically and comprehensively monitor the illegal addition of glucocorticoids in cosmetics is of great significance for ensuring cosmetic quality.

Molecular networking, a non-targeted screening method based on the principle that molecular ions with similar structures produce similar MS/MS fragments, has become an efficient tool for identifying unknown compounds [15-17]. When constructing molecular networks, molecular ions of structurally similar compounds in complex systems are clustered based on the similarity of MS/MS fragments, providing visualized results [15]. Subsequently, known compound nodes can be identified

## \*Corresponding author:

E-mail address: [jhfayy@163.com](mailto:jhfayy@163.com) (J. Fang)

Received: 15 October, 2024 Accepted: 17 February, 2025 Epub Ahead of Print: 07 April 2025 Published: 17 April 2025

DOI: 10.25259/AJC\_85\_2024

using public or self-built MS databases, while unknown compound nodes can be quickly identified by the structural characteristics of known nodes in the same molecular cluster [17]. In the development of the molecular networking technology, a “seed”-based molecular networking strategy has been vigorously developed. The concept of “seed” refers to the introduction of known compounds with well-defined chemical structures and MS characteristics as reference points when constructing molecular networking. By leveraging their structural characteristics and MS data, unknown compounds with similar mass spectral features can be quickly identified, thereby enhancing the accuracy and efficiency of the identification process. This strategy has been applied in fields, such as natural product discovery, environmental pollutant identification, and food analysis [18-20]. For example, Zhu *et al.* used identified polyketones as seeds to discover eight new types of polyketones and elucidate their biosynthetic pathways in the phytopathogenic fungus *Epicoccum nigrum* 09116 [18]. Additionally, integrating known peptides with molecular networking has been used to identify umami peptides in fermented seasoning douchi, ultimately identifying 18 umami peptides, seven of which were previously unreported [20]. Recently, this method has been successfully applied to screen prohibited colorants in cosmetics. Woo *et al.* identified 26 colorants in actual samples beyond the targeted colorants (Disperse Red 17, Disperse Red 1, and Disperse Blue 14) [21]. Thus, using the molecular networking strategy with “seed” nodes is expected to identify more unknown risk substances in the non-targeted screening of glucocorticoids in cosmetics, providing a new approach for screening unknown risk substances in these products.

Proteins are the primary bearers of biological activities, and many diseases are caused by protein mutations [22]. Recently, *in silico* approaches, such as molecular docking and molecular dynamics (MD) simulation, have been widely used to study the interactions between small molecules and proteins, revealing the toxicity and mechanism of small molecules [23,24]. In the current work, we aimed to propose an innovative non-targeted screening approach for glucocorticoids in cosmetics using Feature-Based Molecular Networking (FBMN) and explore the potential skin atrophy and endocrine disruption effects of screened glucocorticoids using *in silico* methods. The results of this study are expected to provide new insights into the non-targeted screening and toxicity assessment of glucocorticoids in cosmetics.

## 2. Materials and Methods

### 2.1. Chemicals and materials

A total of 36 glucocorticoid reference standards used to establish the standard method were obtained from Shanghai Aladdin Biochemical Technology Co., Ltd. (Shanghai, China) and National Institutes for Food and Drug Control (Beijing, China), and more information of these reference standards has been provided in Table 1. In addition, the reference standard of clobetasol propionate, halobetasol propionate, betamethasone dipropionate, and prednisone acetate were acquired from Shanghai Maclin Biochemical Technology Co., Ltd. (Shanghai, China). Dexamethasone phosphate (Dex-P) were bought from CATO Research Chemicals Inc. (Guangzhou, China). MS grade acetonitrile, methanol, ammonium acetate and formic acid were bought from Shanghai Macklin Biochemical Technology Co., Ltd. (Shanghai, China). Ultrapure water was obtained from a Milli-Q advantage ultrapure water system (Merck Chemical Co., Ltd.). Seven cosmetic samples (labeled C1-C7) were collected from the online and offline markets, other samples came from supervised sampling tasks. Additionally, these cosmetic categories include repair creams, light printing creams, whitening creams, pore unblocking liquids, and skin brightening essences.

### 2.2. Stock and working solutions

Individual stock solutions of 36 reference standards were prepared with concentration of 1.0 mg/mL using methanol. A mixture working solution with a concentration of 1.0 µg/mL was prepared by diluting the individual standard solutions with acetonitrile. Working solutions of Dex-P were prepared in methanol at a concentration of 1.0 µg/mL. All solutions were stored in the dark at 4°C.

### 2.3. Sample preparation

Approximately 500 mg of each cosmetic samples were measured and placed in a 20 mL stopper colorimetric tube. Next, 3 mL of a saturated sodium chloride solution was added to the tube containing the cosmetics sample and swirled for 1 min to form a uniform solution. Following this, 10 mL of a 0.1% formic acid solution in methanol was meticulously added to the tube, and the mixture was sonicated for 30 mins. After ultrasonication, the samples were centrifuged at a speed of 4000 revolutions per minute (r/min) for a period of 10 min. Finally, 1 mL of the supernatant liquid was carefully pipetted and filtered through a 0.22-micrometer (µm) filter membrane and stored at a temperature of 4°C until further analysis.

### 2.4. Chromatographic and mass spectrometric analysis conditions

Ultra-high performance liquid chromatography - quadrupole time-of-flight mass spectrometry/mass spectrometry (UHPLC-Q-TOF-MS/MS) was performed using an Agilent UPLC system equipped with Agilent G6545 Q-TOF-MS/MS system (Agilent Corp, Santa Clara, USA). Chromatographic separation was performed on a Proshell 120 EC-C18 column (2.1 mm × 100 mm, 1.8 µm) with a column temperature of 25°C. The analytical flow rate was 0.35 mL/min. The mobile phase consisted of acetonitrile (A), a solution of 0.1% formic acid, and 2 mmol/L ammonium acetate (B). The percentage of mobile phase A was linearly varied as follows: 0-1 min, 2%, 1-3 mins, 2%-20%, 3-5 mins, 20%-28%, 5-22 mins, 28%-75%, 22-25 mins, 75%-95%, 25-27 mins, 95%-2%, 27-27.5 mins, 95%-2%, 27.5-30 mins, 2%. The injection volume was precisely set at 5 µL for all assays.

For MS analysis, the analyte was ionized via an electrospray ionization (ESI) source operating in positive mode, and data were acquired in a data-dependent acquisition (DDA) mode. The active exclusion mode was configured as follows: excluded after two spectra and released after 9 s. The temperature of the sheath gas was maintained at 250°C, and that of the drying gas was held at 350°C. The flow rate of the sheath gas was set at 10 L/min, and that of the drying gas was 8 L/min. The voltage of spray and capillary were 500 V and 4.0 kV, respectively. The collision voltage was set within the range of 10 to 40 V, and the non-targeted MS/MS mode was adjusted to analyze the top 5 ions.

### 2.5. Molecular networking analysis

Non-targeted screening of glucocorticoids was performed using FBMN workflow and data mining techniques [19, 20]. The FBMN analysis was conducted based on the cloud-based global natural products social molecular networking platform (GNPS) (<https://gnps.ucsd.edu/>) [15]. Briefly, the raw data from UPLC-Q-TOF-MS/MS analysis were converted into the mzML format using ProteoWizard MSConvert software, while peak picking was performed, followed by data pre-processing, which included data collection, peak detection, peak deconvolution, and peak alignment; completed by MS-DIAL 4.9.221218 [25]. The detailed parameters of MS-DIAL were as follows: minimum peak height set as 5000, mass slice width set as 0.01, MS1 tolerance set as 0.01 Da, MS2 tolerance set as 0.025 Da, sigma window value set as 0.5, tolerance of retention time (RT) set as 0.05 min. Subsequently, the pre-processed data files were subsequently uploaded to the GNPS webserver for molecular networking construction. It is important to emphasize that the MS data of the 36 standards were integrated with the MS data of seven sets of actual samples when obtaining the data files uploaded to GNPS so as to enable efficient clustering based on 36 known compounds when building molecular networking. For molecular networking parameters, the maximum mass tolerances of the parent ions and fragment ions were set to 0.02 Da and 0.02 Da, respectively, and the minimum cosine score and minimum matched peaks to 0.7 and 5, respectively. Other parameters were set as default. Finally, the molecular networking construction result was visualized using Cytoscape V3.7.1.

### 2.6. Data mining strategy

The structural identification of glucocorticoids in cosmetics mainly integrated MS-DIAL, MS-FINDER 3.52, and molecular networking

**Table 1.** Basic and fragmentary information for 36 reference standards.

Number	Compound	CAS Number	Formula	RT/min	[M+H] <sup>+</sup>	Fragments
1	Triamcinolone	124-94-7	C <sub>21</sub> H <sub>27</sub> FO <sub>6</sub>	6.469	395.1864	375.1805, 357.1685, 339.1585, 321.1476, 311.1636, 237.1262, 225.1273, 185.0956, 135.0812, 147.0802, 121.0631
2	Prednisolone	50-24-8	C <sub>21</sub> H <sub>28</sub> O <sub>5</sub>	7.828	361.201	343.1899, 325.1823, 307.1691, 289.1589, 279.1732, 239.1438, 223.1116, 173.0953, 147.0808, 121.0620
3	Prednisone	53-03-2	C <sub>21</sub> H <sub>26</sub> O <sub>5</sub>	7.881	359.1853	341.1740, 323.1628, 313.1794, 305.15364, 295.1686, 283.1714, 277.1578, 265.1590, 237.1260, 147.0793, 135.0801
4	9-Fluoroprednisolone	338-95-4	C <sub>21</sub> H <sub>27</sub> FO <sub>5</sub>	7.902	379.1945	359.1851, 341.1746, 323.1641, 305.1536, 237.1272, 171.0801, 147.0806, 135.0795, 121.0641
5	Hydrocortisone	50-23-7	C <sub>21</sub> H <sub>30</sub> O <sub>5</sub>	7.960	363.2166	345.2049, 327.1961, 309.1842, 291.1733, 297.1857, 281.1896, 267.1740, 257.1534, 147.11577, 135.0792, 121.0643
6	Cortisone	53-06-5	C <sub>21</sub> H <sub>28</sub> O <sub>5</sub>	8.116	361.201	343.1936, 325.1765, 301.1782, 295.1687, 267.1745, 163.1118, 147.0789, 135.0805, 121.0654
7	Methylprednisolone	83-43-2	C <sub>22</sub> H <sub>30</sub> O <sub>5</sub>	9.113	375.2166	357.2057, 339.1952, 321.1849, 303.1733, 279.1736, 253.1578, 211.1114, 185.0963, 161.0963, 135.0798, 121.0643
8	Betamethasone	378-44-9	C <sub>22</sub> H <sub>29</sub> FO <sub>5</sub>	9.354	393.2048	373.2004, 355.1903, 337.1794, 319.168, 309.1853, 279.1736, 161.0964, 147.0799,
9	Dexamethasone	50-02-2	C <sub>22</sub> H <sub>29</sub> FO <sub>5</sub>	9.477	393.2073	373.2004, 355.1903, 337.1794, 319.168, 309.1853, 279.1736, 161.0964, 147.0799
10	Flumethasone	2135-17-3	C <sub>22</sub> H <sub>28</sub> F <sub>2</sub> O <sub>5</sub>	9.587	411.1978	391.1905, 371.1847, 353.1727, 335.1642, 307.1677, 277.1586, 253.1215, 235.1109, 147.0786, 135.0802, 121.0653
11	Beclomethasone	4419-39-0	C <sub>22</sub> H <sub>29</sub> ClO <sub>5</sub>	9.883	409.1776	391.1667, 373.2008, 355.1896, 337.1795, 319.1686, 279.1741, 263.1423, 237.1265, 173.0960, 147.0804, 135.0812
12	Triamcinolone acetonide	76-25-5	C <sub>24</sub> H <sub>31</sub> FO <sub>6</sub>	10.122	435.2177	415.2100, 397.2008, 357.1689, 339.1585, 321.1482, 311.1631, 293.1531, 263.1417, 225.1271, 171.0805, 147.0805, 121.0638
13	Desonide	638-94-8	C <sub>24</sub> H <sub>32</sub> O <sub>6</sub>	10.089	417.2272	399.2164, 341.1750, 323.1639, 295.1703, 265.1591, 225.1275, 173.0980, 147.0805, 121.0678
14	Flunisolide	77326-96-6	C <sub>24</sub> H <sub>31</sub> FO <sub>6</sub>	10.285	435.2177	415.2100, 397.2008, 357.1689, 339.1585, 321.1482, 293.1531, 263.1417, 237.1275, 225.1271, 171.0805, 147.0805, 121.0638
15	Fluoromethaolone	426-13-1	C <sub>22</sub> H <sub>29</sub> FO <sub>4</sub>	11.032	377.2123	357.2056, 339.1956, 321.1845, 303.1734, 297.1852, 279.1738, 251.1424, 237.1277, 229.1208, 161.0954, 135.0816
16	Halometasone	50629-82-8	C <sub>22</sub> H <sub>27</sub> ClF <sub>2</sub> O <sub>5</sub>	11.625	445.1588	427.1472, 387.1340, 357.1250, 349.1340, 341.1285, 307.0889, 287.0810, 275.1415, 257.0730, 161.0955, 155.0260
17	Budesonide	51333-22-3	C <sub>25</sub> H <sub>34</sub> O <sub>6</sub>	12.567	431.2428	413.2321, 341.1749, 323.1643, 305.1518, 295.1698, 239.1420, 223.1110, 173.0963, 147.0796, 121.0656
18	Fluocinolone acetonide	67-73-2	C <sub>24</sub> H <sub>30</sub> F <sub>2</sub> O <sub>6</sub>	10.593	453.2083	433.2026, 413.1953, 355.1536, 337.1426, 319.1335, 291.1368, 277.1214, 253.1220, 241.1209, 121.0645
19	Fluocinonide	356-12-7	C <sub>26</sub> H <sub>32</sub> F <sub>2</sub> O <sub>7</sub>	14.609	495.2189	475.2118, 455.2063, 357.1492, 337.1435, 319.1319, 309.1486, 291.1378, 279.1380, 253.1223, 135.0798, 121.0633
20	Halcinonide	3093-35-4	C <sub>24</sub> H <sub>32</sub> ClFO <sub>5</sub>	16.214	455.1995	359.1427, 337.1375, 283.0895, 265.1595, 227.1424, 181.1014, 161.0957, 143.0857, 121.0647
21	Amcinonide	51022-69-6	C <sub>28</sub> H <sub>35</sub> FO <sub>7</sub>	16.600	503.244	483.2378, 399.1796, 339.1588, 321.1483, 311.1624, 293.1519, 275.1441, 233.1114, 173.0956
22	Paramethasone	53-33-8	C <sub>22</sub> H <sub>29</sub> FO <sub>5</sub>	9.456	393.2073	373.2004, 355.1903, 337.1794, 319.168, 309.1853, 279.1736, 161.0964, 147.0799, 135.0915
23	Triamcinolone diacetate	67-78-7	C <sub>25</sub> H <sub>31</sub> FO <sub>8</sub>	10.623	479.2076	459.2005, 441.1900, 339.1599, 321.4886, 311.1632, 303.1376, 293.1538, 279.1384, 263.1426, 187.0751, 147.0813, 121.0648
24	Prednisolone acetate	52-21-1	C <sub>23</sub> H <sub>30</sub> O <sub>6</sub>	10.723	403.2115	385.2007, 325.1785, 307.1692, 289.1582, 279.1742, 147.0803, 135.0800, 121.0646
25	Hydrocortisone acetate	50-03-3	C <sub>23</sub> H <sub>32</sub> O <sub>6</sub>	10.950	405.2272	327.1957, 309.1843, 291.1738, 281.1902, 241.1589, 173.0948, 147.0797, 135.0797, 121.0647
26	Fludrocortisone acetate	514-36-3	C <sub>23</sub> H <sub>31</sub> FO <sub>6</sub>	11.114	423.2177	405.2079, 343.1900, 325.1802, 279.1724, 257.1531, 181.1020
27	Cortisone acetate	50-04-4	C <sub>23</sub> H <sub>30</sub> O <sub>6</sub>	11.605	403.2115	385.2003, 343.1905, 325.1803, 307.1688, 163.1113, 121.0650
28	Methylprednisolone acetate	53-36-1	C <sub>24</sub> H <sub>32</sub> O <sub>6</sub>	12.164	417.2272	399.2163, 339.1957, 321.1848, 303.1732, 293.1879, 279.1740, 253.1583, 161.0949, 135.0806, 121.0656
29	Betamethasone acetate	987-24-6	C <sub>24</sub> H <sub>31</sub> FO <sub>6</sub>	12.281	435.2177	415.2101, 397.2005, 355.1903, 337.1797, 319.1686, 309.1846, 279.1758, 237.1278, 161.09605, 147.0804, 135.0787
30	Dexamethasone acetate	1177-87-3	C <sub>24</sub> H <sub>31</sub> FO <sub>6</sub>	12.725	435.2177	415.2101, 397.2005, 355.1903, 337.1797, 319.1686, 309.1846, 291.1733, 279.1758, 237.1278, 227.1426, 147.0804
31	Hydrocortisone butyrate	13609-67-1	C <sub>25</sub> H <sub>36</sub> O <sub>6</sub>	12.720	433.2585	345.2055, 327.1940, 309.1843, 279.1765, 267.1735, 121.0652
32	Fluorometholone acetate	3801-06-7	C <sub>24</sub> H <sub>31</sub> FO <sub>5</sub>	13.255	419.2228	399.2151, 339.1941, 321.1846, 297.1833, 279.1741, 237.1289, 185.0955, 161.0950, 135.0802
33	Hydrocortisone valerate	57524-89-7	C <sub>26</sub> H <sub>38</sub> O <sub>6</sub>	14.269	447.2741	345.2053, 327.1953, 297.1846, 267.1746, 249.1630, 187.1114, 169.1014, 147.0806, 135.0818, 121.0645
34	Triamcinolone acetonide acetate	3870-07-3	C <sub>26</sub> H <sub>33</sub> FO <sub>7</sub>	14.294	477.2283	457.2211, 439.2106, 339.1582, 321.1485, 311.1636, 293.1525, 281.1517, 265.1576, 223.1093, 187.0754, 147.0807
35	Betamethasone valerate	2152-44-5	C <sub>27</sub> H <sub>37</sub> FO <sub>6</sub>	15.498	477.2647	457.2561, 355.1903, 337.1794, 319.1683, 309.1856, 279.1742, 187.0757, 171.0806, 135.0800
36	Betamethasone-17-butyrate-21-propionate	5534-02-1	C <sub>29</sub> H <sub>39</sub> FO <sub>7</sub>	18.814	519.2731	449.2334, 429.2271, 355.2279, 337.1798, 319.1692, 309.1849, 291.1743, 279.1743, 237.1274, 153.0910, 107.0825

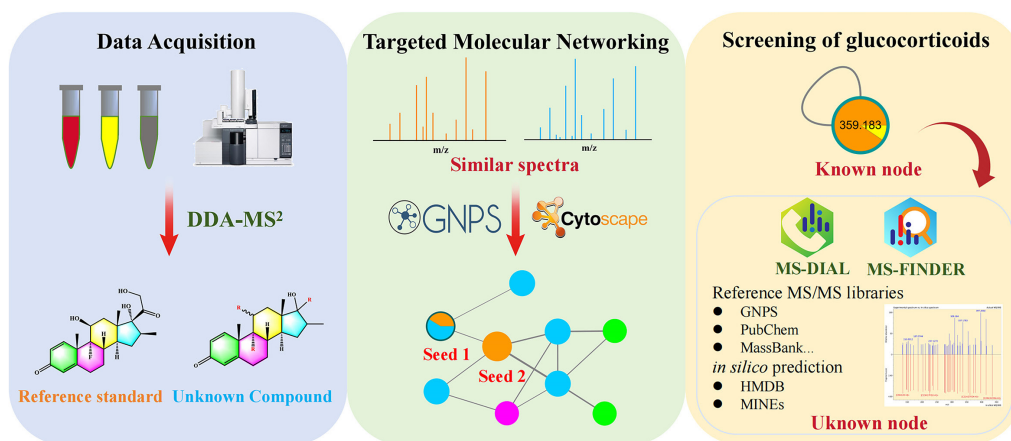


Figure 1. Workflow demonstrating the profiling and annotation of glucocorticoids.

analysis. The process began by quickly localizing the seeds of the 36 known reference standards to molecular clusters and individual nodes associated with glucocorticoids. Then, after entering the precursor ion and RT of the unknown node via MS-DIAL, the information of the unknown node was associated with MS-FINDER for structural annotation. A summary of the analytical workflow, including data acquisition, annotation, and interpretation, has been presented in Figure 1.

During the structure annotation process, MS-DIAL efficiently identifies precursor peaks with enhanced clarity by performing sophisticated deconvolution of the MS/MS spectra, effectively reducing background noise, and precisely extracting spectra from complex mixtures that contain unknown compounds [26]. The corresponding parameters, such as compound composition (e.g., C, H, O, N, F, and Cl atoms), number of candidate substances, and the search scope of database (e.g., GNPS, PubChem, DrugBank, and MINEs), were set in MS-FINDER [26,27]. Through the internal algorithm in MS-FINDER, scores reflecting the similarity between potentially matched compounds and candidate compounds in the database were calculated. The identification of candidate compounds was then determined based on these scores, alongside the fit of the MS/MS spectra,  $m/z$  tolerance, elemental composition, chemical valence rules, and elemental ratios [27]. Moreover, the outcomes of candidate compound identification were classified into four levels of confidence, as detailed in Table S1 [28]. To address the potential sources of error caused by using it in data mining and analysis, we use three factors to analyze the results: fragment similarity, mass error, and identification confidence level.

## 2.7. Molecular docking and molecular dynamics simulations

The ability of glucocorticoids to cause skin atrophy and endocrine disruption was evaluated by molecular docking and dynamics on the active site of hyaluronan synthase 2 (HAS-2) and glucocorticoid receptor (GR) identified using Biovia Discovery studio 4.5 (BIOVIA, 2024), respectively. Structure of HAS-2 of *Homo sapiens* was obtained from AlphaFold Protein Structure Database (<https://www.alphafold.ebi.ac.uk/>) [29,30]. The structure of human GR (PDB id, 4UDC) was selected from the Protein Data Bank [23]. The 3D structure of glucocorticoids and energy minimization were constructed using ChemDraw 19.0. Molecular docking of the ligand and protein was applied through using CDOCKER program of Discovery studio 4.5. Hydrogen bonding and other interactions between the ligand and protein were visualized using Discovery Studio 4.5 and PyMol.

The Dex-P-HAS-2 complex and Dex-P-GR complex with best binding conformations were selected for further MD simulation. The two Dex-P-protein complexes were solvated in orthorhombic cells, where 0.145 mol/L sodium chloride was placed randomly to achieve electrostatic neutrality. The simulation system carried out the energy minimization and equilibrium processes at constant temperature and constant pressure, respectively. After 50 ns dynamics simulation, the Root Mean Squared Deviation (RMSD) values, Root Mean Square Fluctuation (RMSF) values, Radius

of gyration (Rg), key residues, and structural changes for Dex-P-protein were calculated, respectively.

## 3. Results and Discussion

### 3.1. Acquisition of “seed” data by UPLC-Q-TOF-MS/MS

For structure elucidation, known compounds were initially identified as “seed” nodes, which aid in inferring the structures of adjacent nodes [19,20]. A mixture of 36 reference standards, each at a concentration of 1.0  $\mu\text{g/L}$ , was analyzed using UPLC-Q-TOF-MS/MS to obtain the “seed” data. Details of the 36 reference standards have been summarized in Table 1. Total ion chromatograms (TICs) of 36 reference standards have been displayed in Figure S1, and the MS/MS spectra of every standard have been shown in Figures S2-S4.

As indicated in Table 1, several fragment ions appeared frequently among the reference standards, notably at  $m/z$  355 ( $[\text{C}_{22}\text{H}_{26}\text{O}_4]^+$ ), 337 ( $[\text{C}_{22}\text{H}_{25}\text{O}_3]^+$ ), 319 ( $[\text{C}_{22}\text{H}_{23}\text{O}_2]^+$ ), 309 ( $[\text{C}_{21}\text{H}_{20}\text{O}_2]^+$ ), and 237 ( $[\text{C}_8\text{H}_9\text{N}_2\text{O}_2]^+$ ). Chen *et al.* utilized these characteristic ions, particularly those at  $m/z$  355, 337, and 319, to annotate the structures of betamethasone dibutyrate and betamethasone tributrylate [31]. Approximately half of the glucocorticoids showed a common fragment ion at  $m/z$  279 ( $[\text{C}_{20}\text{H}_{23}\text{O}]^+$ ), which Karakka Kal *et al.* noted as a key characteristic ion of fluorometholone [32]. Similarly, Kim *et al.* observed this fragment ion in the structural fragments of beclomethasone, clobetasone butyrate, and mometasone furoate [11]. Additionally, fragment ions at  $m/z$  355, 337, 319, 309, 279, and 237 were present in the fragmentation pathways of betamethasone, and dexamethasone [33]. Moreover, most glucocorticoids contained fragment ions at  $m/z$  147, 135, and 121, which corresponded to the identity of  $[\text{C}_{11}\text{H}_{15}]^+$ ,  $[\text{C}_{10}\text{H}_{15}]^+$ , and  $[\text{C}_8\text{H}_9\text{O}]^+$ , respectively. This observation is consistent with the MS analysis of steroid structures conducted by Jian *et al.* [10]. Furthermore, Yang *et al.* found that clobetasol propionate contained the characteristic ions at  $m/z$  147 and 121 [34]. In all, the MS/MS spectra of known glucocorticoids provide valuable structural information about compounds, and the presence of shared fragment ions facilitates the grouping and classification of similar compounds.

### 3.2. Identification of glucocorticoids using the “seed” molecular networking strategy

The integration of FBMN with UPLC-Q-TOF-MS/MS provides a rapid and efficient approach for the non-targeted screening of unknown compounds [19,20]. To efficiently identify unknown glucocorticoids, data from 36 reference standards were utilized as “seed” to construct molecular networking specific to glucocorticoids with seven cosmetic products (Figure S5). Each node in the molecular network corresponds to a unique feature molecule. As illustrated in Figure 2(a-d), the color of each node indicates the relative abundance of the compound in different groups: orange represents known reference standards used as seeds, grey indicates unidentified compounds, and other colors denote compounds identified using MS-DIAL/MS-FINDER. Consequently, a

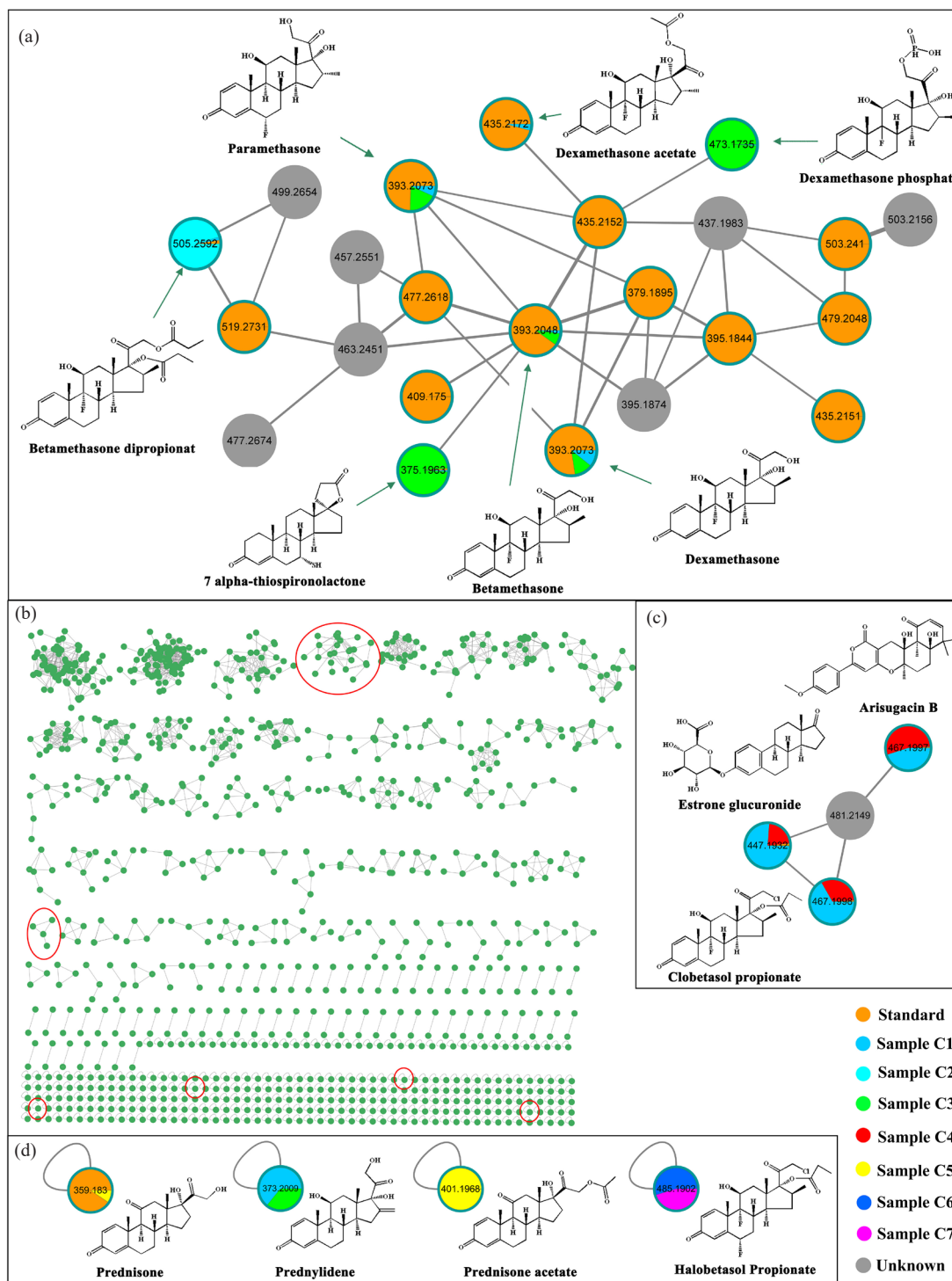


**Figure 2.** Molecular networking of all components in seven cosmetics and 36 reference standards. (a) A glucocorticoid-related molecular cluster of 27 nodes. (b) Results of 129 molecular networking clusters and partial single node. (c) A glucocorticoid-related molecular cluster of four nodes. (d) Four single node of glucocorticoid. Label of node refers to  $m/z$ , and the width of wire refers to the cosine score of fragment ions between neighboring nodes. The red circles represent molecular clusters and single nodes associated with glucocorticoids.

total of 37,724 positive precursor ions from actual samples, along with 36 reference standards, were organized into 129 clusters (nodes  $\geq 2$ ) and 36,939 single nodes (Figure S6).

### 3.2.1. Known glucocorticoids identified via reference methods

Compounds with similar MS/MS fragmentation patterns tend to form molecular families [20]. Utilizing “seed” compounds as indicators, we rapidly identified a glucocorticoid-related molecular cluster

comprising 27 nodes, alongside a single glucocorticoid node among 36,939 individual nodes (Figure 2b-d).

As illustrated in Figure 2(b), betamethasone ( $m/z$  393.2048, RT 9.368 min), paramethasone ( $m/z$  393.2073, RT 9.456 min) and dexamethasone ( $m/z$  393.2073, RT 9.516 min) were included in the “seed” data. From the visualization spectra, it was evident that all three compounds were present in samples C1 and C3. In addition, the “seed” compound dexamethasone acetate ( $m/z$  435.2172, RT 12.766 min) was found in the same molecular clusters, primarily detected in sample C1. Moreover, the single node compound, prednisone ( $m/z$

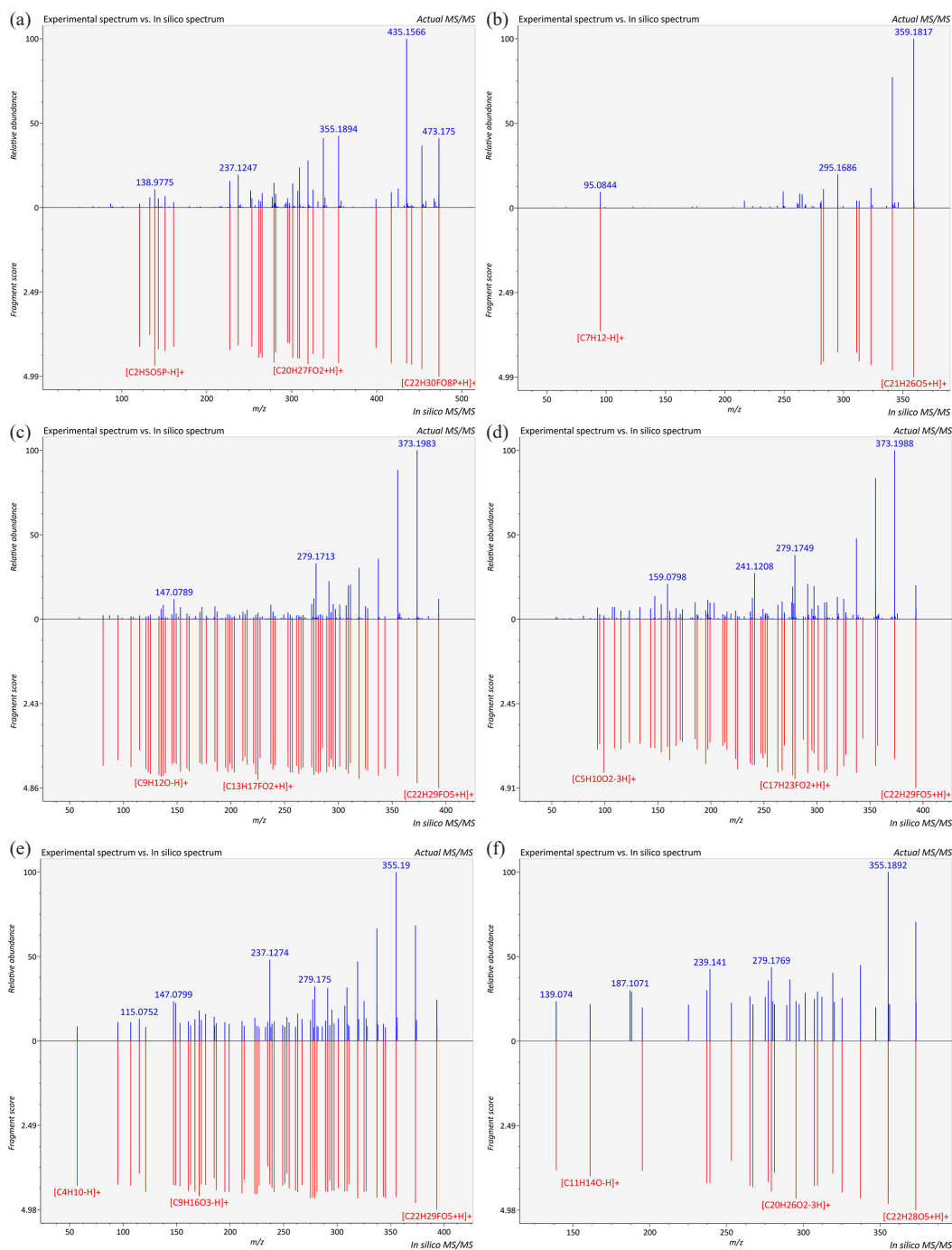


**Figure 3.** Experimental and virtual MS/Mass spectrometry spectra of glucocorticoids. (a) Dex-P, (b) prednisone, (c) betamethasone, (d) paramethasone, (e) dexamethasone, (f) prednylidene.

359.1830, RT 7.896 min), was identified in sample C5 (Figure 2d). The reliability of these identifications was further validated by matching experimental and theoretical fragment ions using MS-FINDER (Figure 3 and S7). According to the confidence levels of identification, these three compounds were considered as level 1 (Table S1) [28]

### 3.2.2. Unknown glucocorticoids identified outside the reference methods

The structural analysis of adjacent unknown nodes was conducted based on the known structures of glucocorticoids. By integrating visualized molecular clusters with the application of MS-DIAL/MS-FINDER, similar glucocorticoid structures were identified through the automatic matching of MS/MS spectra of unknown compounds to databases [26,27].

As illustrated in Figure 2(b) and 3(a), an unknown node in sample C3 was adjacent to betamethasone acetate ( $m/z$  435.2152). Both compounds shared fragment ions at  $m/z$  355, 337, 319, 279, and 237, and it could be identified as dexamethasone phosphate (Dex-P,  $m/z$  473.1735, RT 7.014 min). Salem *et al.* reported fragment ions for Dex-P at  $m/z$  435 ([C<sub>22</sub>H<sub>28</sub>O<sub>5</sub>P]<sup>+</sup>), 355, 337, and 319, which coincided with our findings, and the identification confidence level of Dex-P was classified as level 2a (Table S1) [35]. Furthermore, the unknown node in sample C2 was adjacent to the “seed” node of betamethasone-17-butyrate-21-propionate ( $m/z$  519.2731). They shared the same fragment ions at  $m/z$  355, 337, 319, and 279, leading to the inference that this unknown compound was betamethasone dipropionate ( $m/z$  505.2592, RT 17.529 min) (Figure S8). Specifically, the identification of betamethasone dipropionate was confirmed by a standard substance, classifying it as

**Table 2.** Information on the identified glucocorticoids in seven cosmetics through non-targeted screening based on molecular networking.

Number	Name	Formula	RT/min	Observed m/z	Theoretical m/z	ppm	Fragments	Adduct	Level
1	Dexamethasone phosphate	C <sub>22</sub> H <sub>30</sub> FO <sub>8</sub> P	7.014	473.1735	473.1741	-1.27	473.175, 453.1659, 435.1566, 417.1511, 355.1894, 337.1815, 319.1686, 279.1775, 237.1247	[M+H] <sup>+</sup>	2a
2	Prednisone	C <sub>21</sub> H <sub>26</sub> O <sub>5</sub>	7.896	359.1856	359.1853	-0.83	359.1817, 341.1731, 323.1647, 295.1686, 283.1667, 249.1201, 216.4573	[M+H] <sup>+</sup>	1
3	Betamethasone	C <sub>22</sub> H <sub>29</sub> FO <sub>5</sub>	9.368	393.2072	393.2072	0	393.2048, 373.1983, 355.1875, 337.1775, 319.1661, 279.1713, 277.1566, 161.0952, 159.0798, 147.0798, 121.0662, 107.0851	[M+H] <sup>+</sup>	1
4	Paramethasone	C <sub>22</sub> H <sub>29</sub> FO <sub>5</sub>	9.456	393.2073	393.2071	-0.50	393.2111, 373.1988, 355.1906, 337.1807, 319.1677, 279.1749, 277.1573, 161.0941, 159.0798, 147.0797, 107.0836	[M+H] <sup>+</sup>	1
5	Dexamethasone	C <sub>22</sub> H <sub>29</sub> FO <sub>5</sub>	9.516	393.2073	393.2071	-0.50	393.2055, 373.2004, 319.1686, 279.175, 277.1585, 161.0961, 147.0799	[M+H] <sup>+</sup>	1
6	Prednylidene	C <sub>22</sub> H <sub>28</sub> O <sub>5</sub>	9.516	373.2009	373.2015	-1.61	373.2023, 355.1892, 337.18, 319.1687, 279.1769, 277.1572, 265.1585, 239.1410, 225.1410, 187.1071, 161.0971	[M+H] <sup>+</sup>	2b
7	Prednisone acetate	C <sub>23</sub> H <sub>28</sub> O <sub>6</sub>	11.356	401.1968	401.1958	-2.49	401.1935, 383.1855, 355.1906, 341.1762, 323.1647, 313.1807, 305.1552, 295.1694, 265.1602, 239.1052, 163.0746	[M+H] <sup>+</sup>	1
8	Dexamethasone acetate	C <sub>24</sub> H <sub>31</sub> FO <sub>6</sub>	12.766	435.2172	435.2183	-2.53	435.2165, 415.2109, 397.2002, 355.1878, 337.1783, 319.1703, 279.1743, 277.1572, 187.0744, 161.0974, 147.082, 135.081	[M+H] <sup>+</sup>	1
9	7 alpha-thiospironolactone	C <sub>22</sub> H <sub>30</sub> O <sub>3</sub> S	13.188	375.1963	375.1988	-6.66	375.1963, 357.1802, 319.1682, 309.1867, 301.155, 291.1744, 281.1881, 253.123, 191.1067, 189.0881, 147.0801, 135.0809, 107.0851	[M+H] <sup>+</sup>	2a
10	Arisugacin B	C <sub>27</sub> H <sub>30</sub> O <sub>7</sub>	16.786	467.1997	467.2064	-14.34	467.2018, 447.1952, 373.1574, 355.1457, 319.1707, 279.1719, 135.0794	[M+H] <sup>+</sup>	3
11	Halobetasol propionate	C <sub>25</sub> H <sub>31</sub> ClF <sub>2</sub> O <sub>5</sub>	16.798	485.1902	485.1901	-0.20	465.184, 429.1601, 391.1466, 389.1513, 371.1411, 317.1527, 279.1386	[M+H] <sup>+</sup>	1
12	Clobetasol propionate	C <sub>25</sub> H <sub>32</sub> ClFO <sub>5</sub>	16.839	467.1998	467.2001	-0.64	467.1938, 447.1912, 373.1558, 355.146, 337.1371, 319.1703, 279.1732, 277.161, 263.1429, 221.0961, 147.0796, 121.0645	[M+H] <sup>+</sup>	1
13	Estrone glucuronide	C <sub>24</sub> H <sub>30</sub> O <sub>8</sub>	16.839	447.1932	447.2013	-18.11	447.1938, 373.1563, 355.1451, 327.15, 253.1573, 187.0748, 161.0975	[M+H] <sup>+</sup>	3
14	Betamethasone dipropionat	C <sub>28</sub> H <sub>37</sub> FO <sub>7</sub>	17.529	505.2592	505.2602	-1.98	505.2576, 485.2485, 411.2159, 393.204, 355.1872, 337.1790, 319.1691, 301.1560, 279.1755, 147.0802, 135.0812	[M+H] <sup>+</sup>	1

level 1 (refer Figure S9, Subpart Figure S9a). Additionally, the node representing 7 alpha-thiospironolactone ( $m/z$  375.1963, RT 13.188 min) in sample C3 shared the same fragment ions at  $m/z$  319, 309, and 147 with the adjacent “seed” node of betamethasone. Lee *et al.* quantified spironolactone derivatives using the fragment ion at  $m/z$  107.2 ([C<sub>11</sub>H<sub>11</sub>]<sup>+</sup>), which was also observed in 7 alpha-thiospironolactone in our study [36]. This observation further supported the reliability of the 7 alpha-thiospironolactone identification (Level 2a).

Taking the same workflows applied to Dex-P identification, this strategy was also employed for the identification of other compounds. As shown in Figure 2(c), clobetasol propionate ( $m/z$  467.1998, RT 16.839 min), estrone glucuronide ( $m/z$  447.1932, RT 16.839 min), and arisugacin B ( $m/z$  467.1997, RT 16.786 min) were identified within the same molecular cluster and were detected in samples C1 and C4. Sparidans *et al.* reported the fragment ions for clobetasol propionate as 447 (-HF), 373 (-HF, -C<sub>2</sub>H<sub>5</sub>COOH), and 355 (-HF, -C<sub>2</sub>H<sub>5</sub>COOH, -H<sub>2</sub>O), aligning perfectly with our findings (Figure S8) [37]. The identification of clobetasol propionate was further supported by studies conducted by Yang *et al.* and Guo *et al.* [34,38]. Additionally, validation using the reference standard confirmed the presence of clobetasol propionate (Level 1, Figure S10). Adjacent to the clobetasol propionate node, the node at  $m/z$  447.1932 was identified as estrone glucuronide with a mass error of -19.45 Da, and the node at  $m/z$  467.1997 was identified as arisugacin B with a mass error of -15.635 Da (Figure 3a). Given that the mass errors exceeded the requirement of 10 ppm [39], the confidence level of identification for estrone glucuronide and arisugacin B was considered as level 3.

Furthermore, a single node with an  $m/z$  of 373.2009 was proposed as prednylidene ( $m/z$  373.2009, RT 9.516 min), showing characteristic fragments at  $m/z$  355, 337, 319, and 279 (Figure 2d), and this identification was classified as level 2b (Table S1). Another single node with an  $m/z$  of 401.1925 was identified as prednisone acetate (RT 11.356 min), with main fragments corresponding to 341.1751 [C<sub>21</sub>H<sub>25</sub>O<sub>4</sub>]<sup>+</sup>, 323.1652 [C<sub>21</sub>H<sub>23</sub>O<sub>3</sub>]<sup>+</sup>, 313.1797 [C<sub>20</sub>H<sub>25</sub>O<sub>3</sub>]<sup>+</sup>, 305.1541 [C<sub>18</sub>H<sub>25</sub>O<sub>4</sub>]<sup>+</sup>, and 295.1693 [C<sub>20</sub>H<sub>23</sub>O<sub>2</sub>]<sup>+</sup>. These characteristic ions were consistent with the findings of Guo *et al.* [38], as well as the reference standards (Level 1, Figure S9b). A single node with an  $m/z$  of 485.1902 was identified as halobetasol propionate (RT 16.798 min), and the characteristic ions at

$m/z$  429.1601 and 389.1513 matched those reported by Karakka Kal *et al.* [32]. Moreover, the fragmentation pattern of halobetasol propionate identified in this study was consistent with the reference standard (Level 1, Figure S11).

The non-targeted screening method based on the “seed” molecular networking technology annotated a total of 14 glucocorticoids in seven samples. Notably, this included Dex-P, prednylidene, and 7 alpha-thiospironolactone, which were not identified by the reference method (Table 2). Previous studies have developed various qualitative and quantitative approaches for determining glucocorticoid concentrations in cosmetics [10,40,41]. For example, Giaccone *et al.* reported an analytical method capable of detecting 10 glucocorticoids [40], while Kim *et al.* established a method to identify 43 glucocorticoids [11]. Meng *et al.* introduced a comprehensive screening method targeting 100 illegal substances, including 40 glucocorticoids [41]. While these methodologies have significantly advanced cosmetic safety monitoring, their primary focus has been on well-known glucocorticoids that are already subject to stringent regulatory oversight [42]. Moreover, conventional methods typically require the use of reference standards for each compound during analysis, which is both resource-intensive and inefficient. Given the structural diversity and complexity of glucocorticoids, the efficient detection of unknown glucocorticoids in cosmetics remains a formidable challenge [12-14]. In contrast to the conventional approaches, the adoption of a “seed” node-centric molecular networking approach can meet the needs of current regulations. This innovative technique eliminates the need for an extensive pre-built standard library, enabling a more simplified and cost-effective workflow for the identification and characterization of unknown glucocorticoids in complex samples.

### 3.3. Structure deduction of unknown glucocorticoids

Based on the three-point rule of compound-induced cleavage mentioned in the literature, including the preferential location of cleavage, the sequence of transition state carbon ion stability and the source of product ion charge stability [33, 43-45], the proposed fragmentation pathway of Dex-P, 7 alpha-thiospironolactone, and prednylidene were conducted in this work to further verify the accuracy

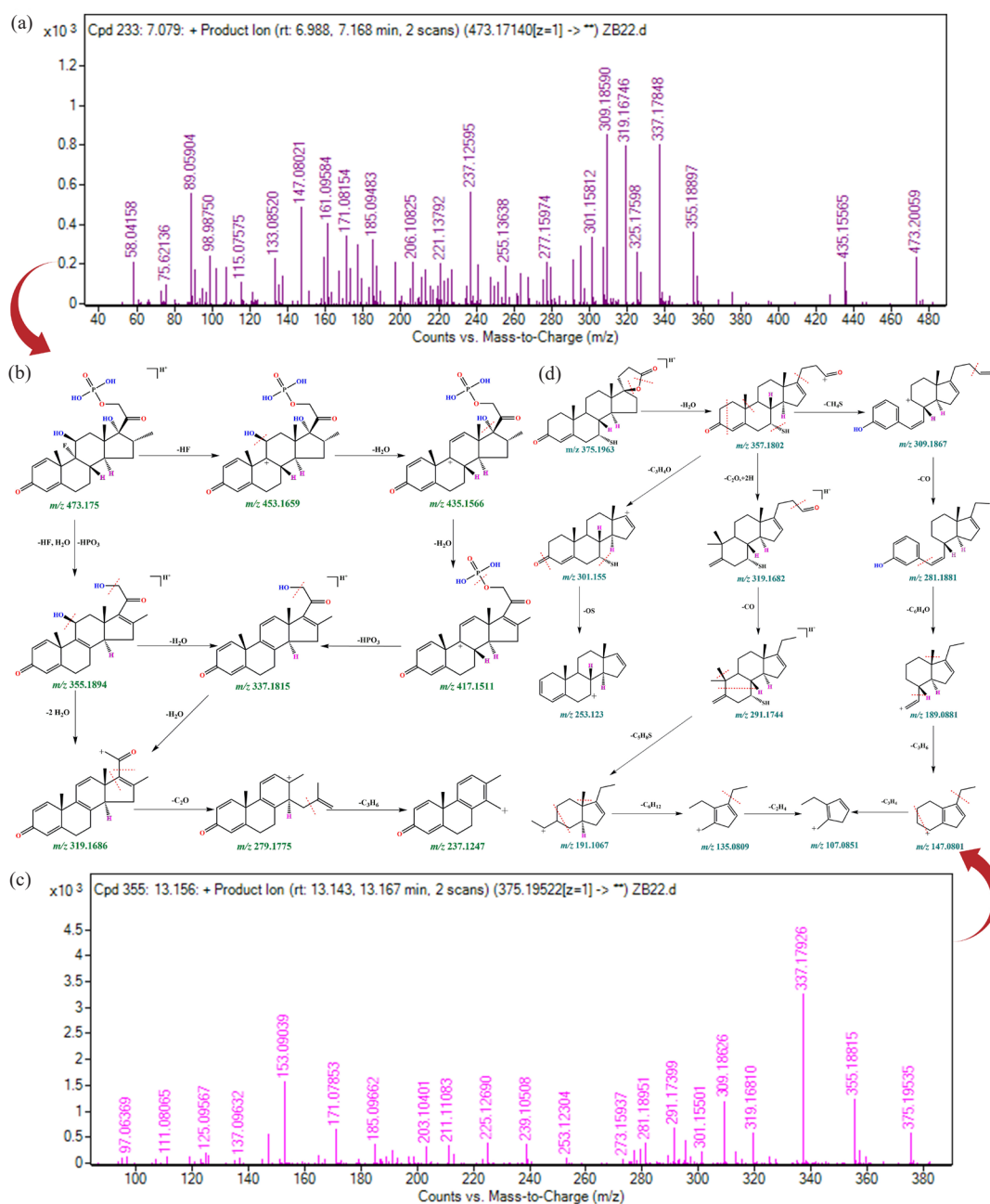


**Figure 4.** Mass spectrometry information and structural annotation results for Dex-P and 7 alpha-thiopyrrolactone. (a) MS/MS spectrometry information of Dex-P, (b) Fragmentation pathway of Dex-P, (c) MS/MS spectrometry information of 7 alpha-thiopyrrolactone, (d) Fragmentation pathway of 7 alpha-thiopyrrolactone.

of the glucocorticoid results identified by MS-DIAL/MS-FINDER. Detailed information on the proposed fragmentation pathways have been presented in Figure 4, and Figure S12.

As seen from the fragmentation pathway of Dex-P ( $m/z$  473.1735) Figure 4(a-b), the first fragment with  $m/z$  453.1659 ( $[M+H-20]^+$ ) was associated with the elimination of HF. With subsequent losses of  $2H_2O$ , fragment ions at  $m/z$  435.1566 ( $[M+H-18]^+$ ) and then  $m/z$  417.1511 ( $[M+H-18]^+$ ) were formed. As reported by Noh *et al.*, loss of HF and  $H_2O$  was a common skeletal fragmentation pathway for betamethasone and dexamethasone and their derivatives [44]. Besides, the fragment ion at  $m/z$  337.1815 ( $[M+H-80]^+$ ) was connected with the loss of  $HPO_3$  from ion at  $m/z$  417.1511. The P-O bond (about 410 kJ/mol) has a higher bond energy than the C-O bond (about 326 kJ/mol), so the loss of  $HPO_3$  was slightly later [46]. Interestingly, the fragment ion at  $m/z$  337.1815 ( $[M+H-18]^+$ ) could be also generated by the ion at  $m/z$  355.1894 from another fragmentation pathway. Moreover, the fragment ion at  $m/z$  319.1686 corresponded with the elimination of  $2H_2O$  ( $[M+H-36]^+$ ) from  $m/z$  355.1894 and  $H_2O$  ( $[M+H-18]^+$ ) from ion at  $m/z$  337.1815,

respectively. Furthermore, the formation of a fragment ion at  $m/z$  279.1775 ( $[M+H-40]^+$ ) was due to the loss of the methyl group and carbonyl group, and the fragment ion at  $m/z$  237.1247 corresponded to the loss of 42 Da attributed to the elimination of  $C_3H_6$ .

As presented in Figure 4(c-d), the fragmentation pathway of 7 alpha-thiopyrrolactone ( $m/z$  375.1963) included the product ions  $m/z$  357.1802, 319.1682, 309.1867, 301.155, 291.1744, 281.1881, 253.123, 191.1067, 189.0881, 147.0801, 135.0809, and 107.0851, respectively. The product resulting from the elimination of  $H_2O$  was a signal with  $m/z$  357.1802 ( $[M+H-18]^+$ ). According to the results of fragmentation ion at  $m/z$  357.1802 possessed three different fragmentation pathways. First, the formation of a fragment ion at  $m/z$  319.1682 ( $[M+H-38]^+$ ) corresponded with the loss of  $C_2O$  and followed by rearrangement. Second, the  $CH_4S$  was lost, resulting in a fragment at  $m/z$  309.1867 ( $[M+H-48]^+$ ). Third, the fragment ion at  $m/z$  301.155 corresponded to the loss of 56 Da attributed to the elimination of  $C_3H_4O$ . The fragment ion at  $m/z$  291.1744 ( $[M+H-28]^+$ ) produced from the ion at  $m/z$  319.1682 corresponds to carbonyl group loss. Concurrent

with this fragmentation channel, the fragment ions at  $m/z$  191.1067 (-100 Da), 135.0809 (-56 Da), and 107.0851 (-28 Da) resulted from the loss of  $C_5H_8S$ ,  $C_6H_{12}$ , and  $C_2H_4$ , respectively. In addition, the fragment ion at  $m/z$  281.1881 had relevance to the elimination of carbonyl group from ion at  $m/z$  319.1682, and the fragment ions at  $m/z$  189.0881 (-92 Da), 147.0801 (-42 Da), and 107.0851 (-40 Da) resulted from the loss of  $C_6H_4O$ ,  $C_3H_6$ , and  $C_3H_6$ , respectively. Moreover, the fragment ion at  $m/z$  253.123 ( $[M+H-48]^+$ ) was associated with the elimination of OS from the ion at  $m/z$  301.155.

As shown in Figure S12, the prednylidene ( $m/z$  373.2009) fragmentation pathway included the product ions  $m/z$  355.1892, 337.18, 319.1687, 279.1769, 277.1572, 265.1585, 239.1410, 225.1410, 187.1071, and 161.0971, respectively. The fragment ions at  $m/z$  355.1892 and 337.18 were both associated with the loss of  $H_2O$ . The  $m/z$  319.1687  $[M+H-18]^+$  and 279.1769  $[M+H-58]^+$  were connected with the loss of hydroxyl and  $C_2H_2O_2$ , respectively. Subsequently, the fragment at  $m/z$  319.1687 formed the fragment ion at  $m/z$  277.1572 and 239.1410, respectively. And then, the fragment ions at  $m/z$  225.1410 and 161.0971 resulted in the loss of  $CH_2$  and  $C_5H_8$ , respectively. In addition, the fragment ions at  $m/z$  265.1585, 225.1410, 187.1071, and 161.0971 corresponded to the loss of  $CH_2$ ,  $C_3H_6$ ,  $C_3H_2$ , and  $C_2H_2$ , respectively. These results not only validate the fragmentation pathways

proposed for Dex-P, 7 alpha-thiospirolactone, and prednylidene but also corroborate the accuracy of the glucocorticoid identification obtained through MS-DIAL/MS-FINDER.

### 3.4. Toxicity prediction of identified glucocorticoids based on molecular docking and molecular dynamics simulations

It is worth emphasizing that unknown glucocorticoids found in the non-targeted screening have not been reported on their potential toxicity or adverse effects, probably because they also have few data on their occurrence. To assess their toxicity, we studied the interaction of glucocorticoids with toxic target proteins.

#### 3.4.1. Ability of glucocorticoids to induce skin atrophy and endocrine disorders

Skin atrophy is a natural aspect of the aging process, but the use of glucocorticoids in skin disease treatment can expedite this progression [47,48]. Studies have shown that dexamethasone reduced hyaluronic acid levels by inhibiting HAS-2 activity in fibroblasts and keratinocytes, thereby contributing to skin atrophy [49]. Herein, the study of the interaction between various glucocorticoids and HAS-2 is helpful in

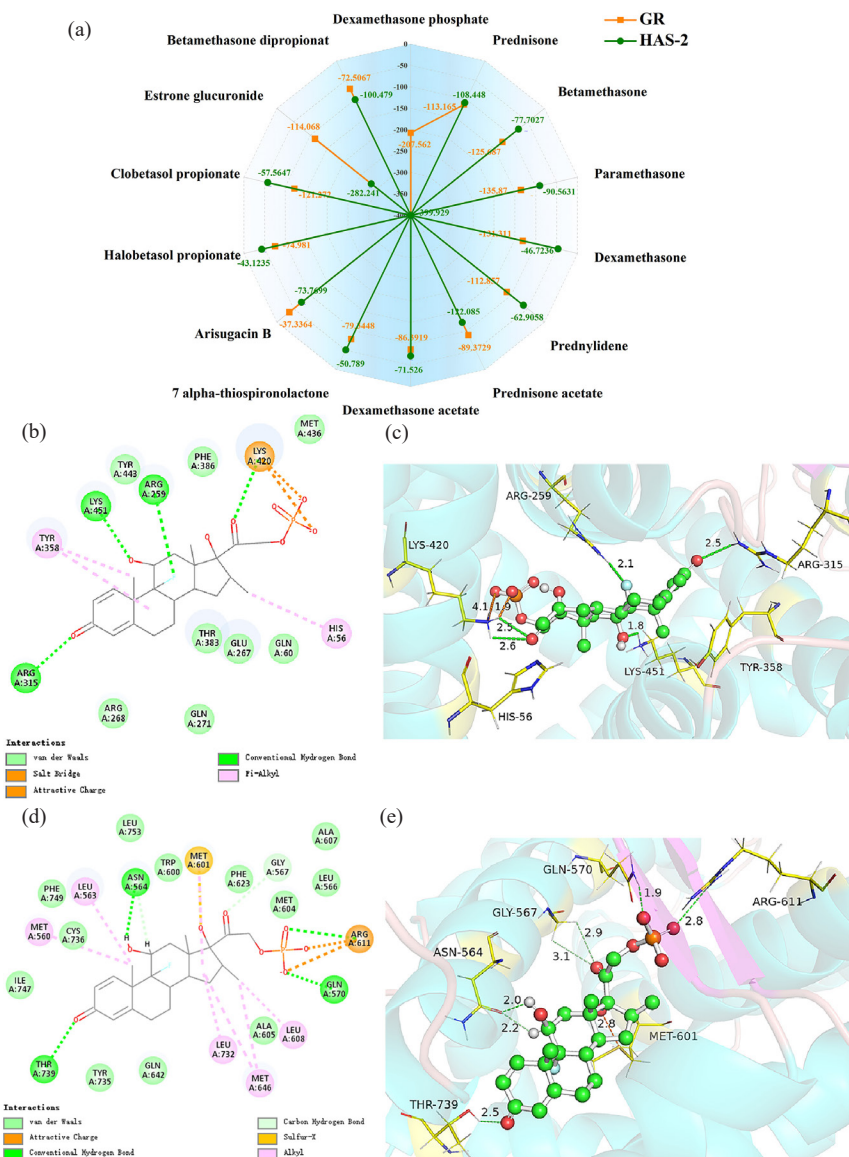


**Figure 5.** Binding energies and interactions of glucocorticoids with HAS-2 and GR. (a) Binding energies (kcal/mol) of all compounds, (b) Two-dimensional interaction diagrams between Dex-P and HAS-2, (c) Three-dimensional interaction diagrams between Dex-P and HAS-2, (d) Two-dimensional interaction diagrams between Dex-P and GR, (e) Three-dimensional interaction diagrams between Dex-P and GR. HAS-2: Hyaluron synthase 2, GR: Glucocorticoid receptor.

understanding the derm-causing capacity of each glucocorticoid. The detailed analysis results are shown in Supplementary Information S1. In Figure 5(a-c) and Table S2, Dex-P showed a strong binding affinity of -399.929 kcal/mol to HAS-2, which is 5.14 to 8.56 times greater than that of dexamethasone and clobetasol propionate. Besides, prednylidene displayed a binding affinity of -62.9058 kcal/mol to HAS-2, surpassing that of dexamethasone (-46.7236 kcal/mol). The binding affinity of 7 alpha-thiospirolactone to HAS-2 was -50.789 kcal/mol, comparable to dexamethasone.

Typically, endocrine disruptors primarily interfere with the endocrine system of organisms by interacting with 12 classical nuclear receptors, such as androgen receptor, estrogen receptor GR, etc., thereby causing adverse developmental, reproductive, neurological, and immune effects [50]. Additionally, exogenous glucocorticoids can mimic endogenous ones by binding to GR, disrupting the endocrine system [6,51]. Therefore, by studying the interaction between different glucocorticoids and GR, we can elucidate their endocrine-disrupting

capabilities. As depicted in Figure 5(d-e), 14 glucocorticoids effectively bound to the ligand-binding domain (LBD) of the GR, like glucocorticoid antagonists such as mifepristone and 3,6-dibromocarbazole [52]. Singh et al. showed that dexamethasone could form hydrogen bonds with the same amino acid residues in the LBD, consistent with our findings [23]. Among these compounds, Dex-P had the strongest binding affinity (-207.562 kcal/mol) (Figure 5a and Table S3). Overall, unknown compounds identified through molecular networking also showed potential for inducing skin atrophy and endocrine disorders, with Dex-P having the greatest potential.

### 3.4.2. Molecular mechanism of skin atrophy and endocrine disorders induced by dexamethasone phosphate

To explore the binding mechanism between Dex-P and the target protein, we performed 50 ns molecular dynamics (MD) simulations. In Figure 6(a-b), RMSD values for the Dex-P-HAS-2 complex increased

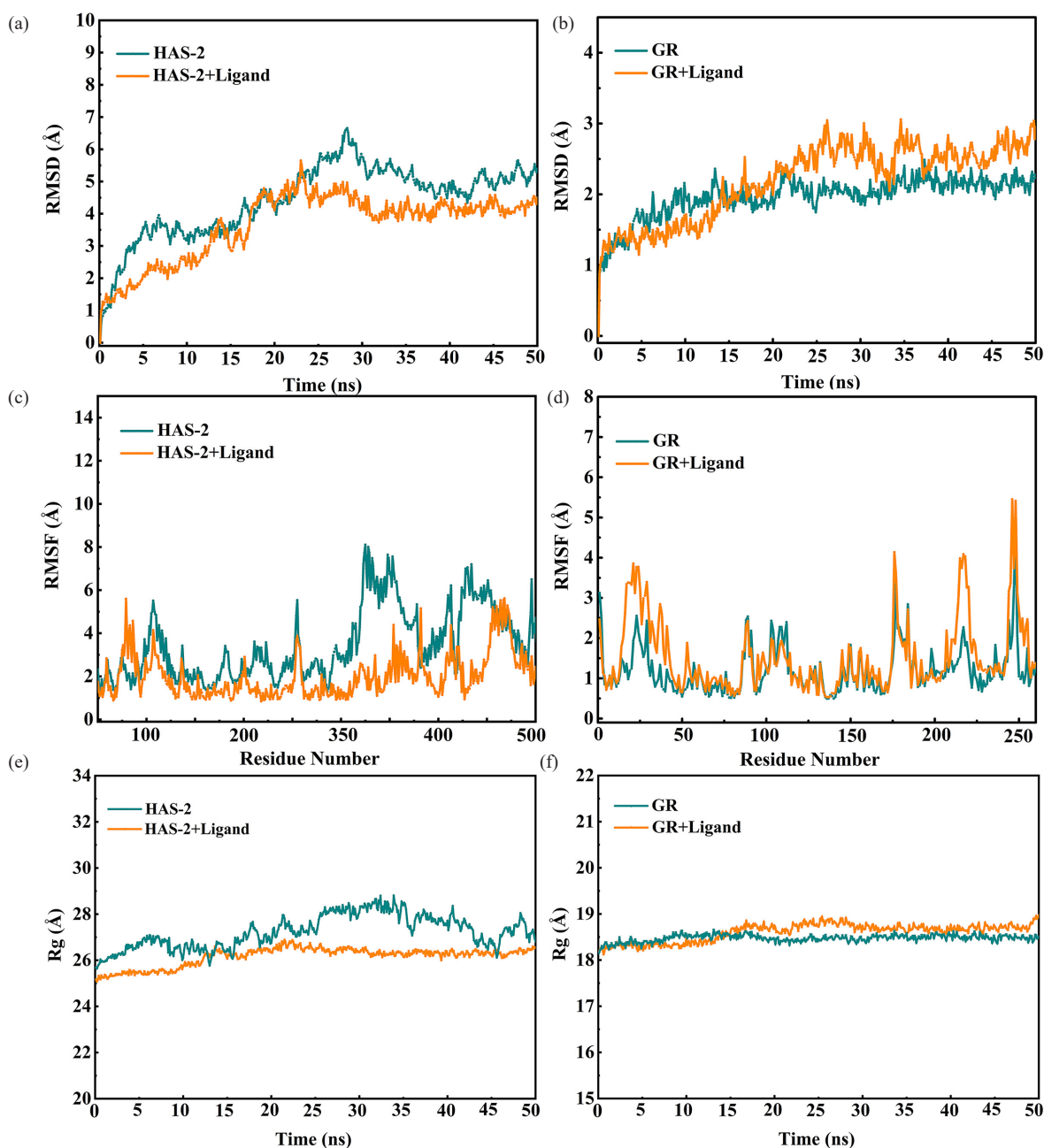


**Figure 6.** Structural dynamics evolution in molecular systems during 50 ns MD simulations. (a) RMSD plot of HAS-2 and Dex-P-HAS-2 complex, (b) RMSD plot of GR and Dex-P-GR complex, (c) RMSF plot of HAS-2 and Dex-P-HAS-2 complex, (d) RMSF plot of GR and Dex-P-GR complex, (e) Rg plot of HAS-2 and Dex-P-HAS-2 complex, (f) Rg plot of GR and Dex-P-GR complex. MD: Molecular dynamics, RMSD: Root mean square deviation, RMSF: Root mean square fluctuation, Rg: Radius of gyration, Dex-P: Dexamethasone-21-phosphate, HAS-2: Hyaluronan synthase 2, GR: Glucocorticoid receptor.

continuously from 0 ns to 30 ns, while for the Dex-P-GR complex, they increased from 0 ns to 25 ns. After this period, RMSD values stabilized, suggesting that the systems had equilibrated. In both protein-ligand complexes, most RMSF were below 3 Å (Figure 6c-d), with residues within 4 Å of the ligand showing values below 2.5 Å (Figure S13). These findings suggested that the Dex-P could stably bind with HAS-2 and GR, respectively. In addition, the Rg value of Dex-P-HAS-2 complex was  $26.16 \pm 0.40$  Å, while that of HAS-2 alone was  $27.23 \pm 0.71$  Å (Figure 6e). The change in Rg value suggested HAS-2 became more compact upon ligand binding. For Dex-P-GR complex, the Rg value was  $18.61 \pm 0.18$  Å compared to  $18.47 \pm 0.08$  Å for GR alone, indicating minimal change in protein compactness and suggesting stable ligand binding (Figure 6f).

Furthermore, we analyzed the frequency of interactions between the ligand and residues in MD simulations and investigated the conformational snapshots of MD trajectory at 0, 30 (25) ns, and 50 ns. In Figure S14, subparts Figures S14a and S14(c-h), ARG315, ARG268, TYR358, ARG259, LYS451, GLU267, and CYS279 occupied prominent positions in Dex-P binding to HAS-2 throughout MD simulation. For the

Dex-P-GR complex, high interaction frequency was observed between Dex-P and residues ARG611, LEU608, LEU563, MET604, ARG569, MET560, and GLN570 during MD simulations (Figure S14b). As shown in Figure S15, the number of hydrogen bonds formed between Dex-P and residues increased from 3 to 4, and then to 6 at 0, 25, and 50 ns. Meanwhile, the interactions between Dex-P and ARG611, LEU563, and GLN570 remained. In short, Dex-P can bind to HAS-2 and GR, thereby inducing changes in protein conformation and altering protein activity. Consequently, Dex-P may affect the skin barrier and endocrine systems of organisms. However, the computer prediction is mainly to predict the possible interactions between proteins and ligands, and some experimental studies are needed to verify the theoretical results in the next step of research.

### 3.5. Qualitative analysis of dexamethasone phosphate in real samples

Based on the toxicity prediction results, the surreptitious addition of Dex-P, a newly identified risk substance, warrants increased scrutiny during the monitoring of actual samples. For this purpose, after acquiring the corresponding reference standard, we conducted

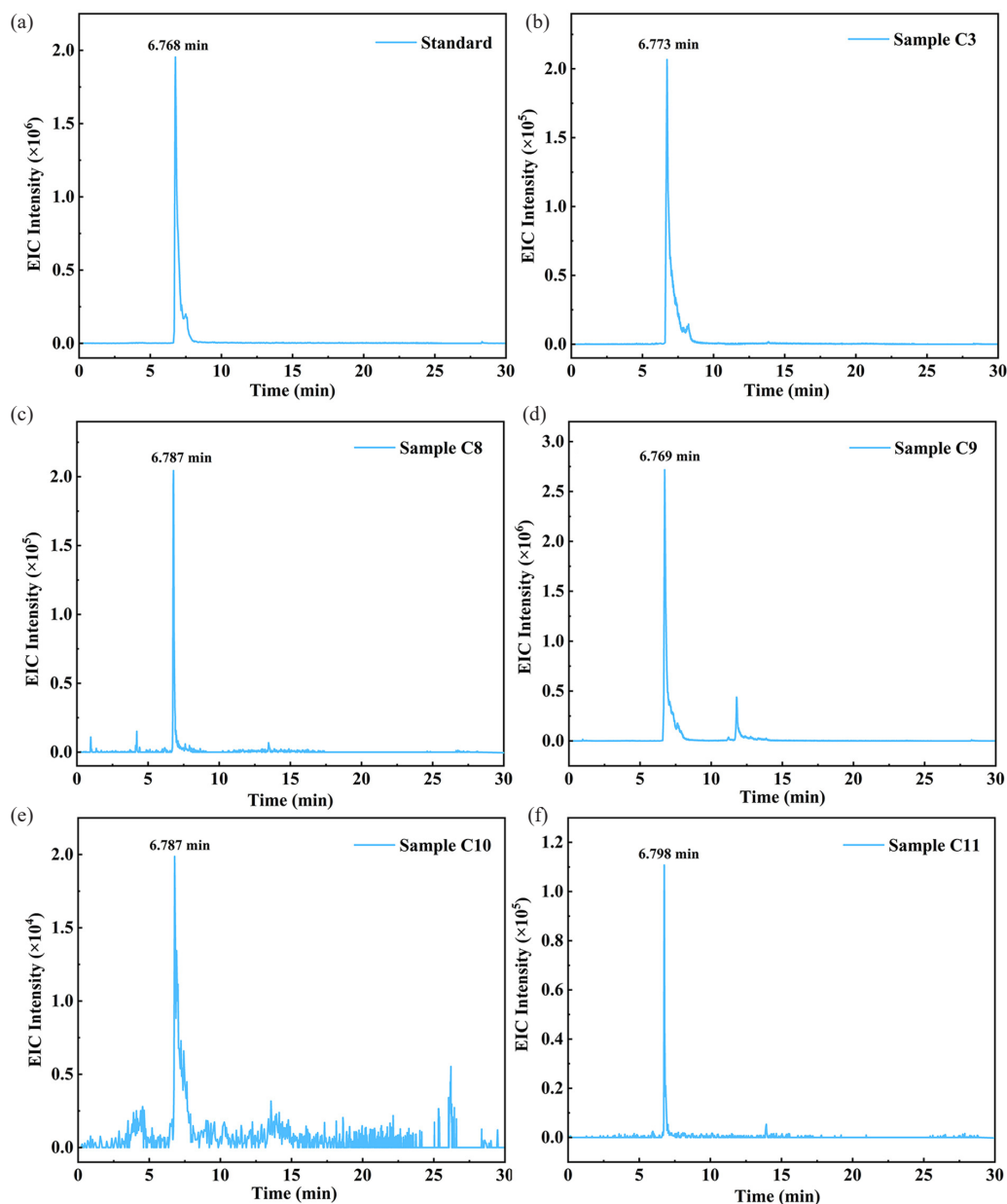


Figure 7. EIC plot of Dex-P in standards and real sample. (a) Dex-P standard; (b) Sample C3; (c) Sample C8; (d) Sample C9; (e) Sample C10; (f) Sample C11. EIC: Extracted ion chromatogram, Dex-P: Dexamethasone-21-phosphate.

tests on both the Dex-P standard and actual samples under identical chromatographic-mass spectrometric conditions to further confirm the presence of Dex-P. As shown in Figure 7(a-b) and S16, the retention time (RT) of the Dex-P standard was consistent with the detection time in sample C3. Additionally, the Dex-P standard exhibited identical fragmentation patterns as observed in the identification results, including  $m/z$  435.1567, 355.1904, 337.1774, 319.1704, and 237.1250 (Figure S17). These findings indicate that the findings from the results obtained from “seed”-based molecular networking were substantiated by the qualitative analysis based on the Dex-P standard.

To broaden our screening efforts, we tested 50 additional batches of actual samples to detect the illegal addition of Dex-P, using the validated results as a reference. In the target screening, Dex-P was detected in four samples, with concentrations varying from 203.35 to 27,810.58 ng/g (Figure 7c-f). The National Medical Products Administration (NMPA) clearly stipulated that hormones, including but not limited to anti-androgen substances of steroid structure, glucocorticoids (corticosteroids), estrogens, palamison, progesterone, substances with androgen effect, etc. were prohibited in cosmetics. In addition, the cosmetic matrices involved in the actual samples of this study include repair creams, light printing creams, pore-unblocking liquids, etc. Woo et al. applied a similar approach to eyebrow tattoos, lipstick tattoos, and hair tint samples [21]. Furthermore, our previous study utilized the FBMN method to screen various actual samples of creams and waters, and screened for antibiotics, antihistamines, phthalates, etc., and these results demonstrated the feasibility of our method for a wide range of cosmetic matrices and repeated regulatory use [53]. Therefore, the use of molecular networking technology for suspicious screening can significantly enhance our efforts to monitor and identify more risk sources in cosmetics in the future.

#### 4. Conclusions

This study established a “seed”-based molecular networking approach for non-targeted glucocorticoid screening in cosmetics, which effectively addressed the limitations of traditional targeted analysis methods in detecting illegal additives. By using 36 known glucocorticoids as “seeds,” 14 glucocorticoids were identified in seven cosmetic products. Among them, five newly discovered substances (Dex-P, prednylidene, and 7 alpha-thiospirolactone, etc.) were further investigated. *In silico* simulations were conducted to assess their toxicity, and results showed that Dex-P had the highest risk of causing skin atrophy and endocrine disruption. The presence of Dex-P was further confirmed by standard reference analysis, and its presence was found in additional actual samples. In conclusion, the findings of this study provide an efficient regulatory approach for glucocorticoids in cosmetics, which has significant implications for the scientific oversight of cosmetic products.

#### CRedit authorship contribution statement

**Dong Guo:** Methodology, Investigation, Writing (original draft). **Yaxiong Liu:** Methodology, Validation. **Jingwen Liang:** Investigation, Validation. **Yayang Huang:** Investigation. **Yangjie Li:** Writing-reviewing and editing. **Qunyue Wu:** Supervision, Funding acquisition. **Sheng Yin:** Supervision, Writing-reviewing and editing. **Jihui Fang:** Supervision, Conceptualization, Funding acquisition.

#### Declaration of competing interest

The authors declare that they have no known competing financial interests or personal relationships that could have appeared to influence the work reported in this paper.

#### Declaration of Generative AI and AI-assisted technologies in the writing process

The authors confirm that they have used artificial intelligence (AI)-assisted technology for assisting in the writing or editing of the manuscript.

#### Acknowledgment

We gratefully acknowledge financial support from the Scientific and technological innovation project of Guangdong Provincial Drug Administration (ZA20230069, 2024ZDZ04), the Science and Technology Plan Project of Guangdong Provincial (2023A1111120025).

#### Supplementary data

Supplementary material to this article can be found online at [https://dx.doi.org/10.25259/AJC\\_85\\_2024](https://dx.doi.org/10.25259/AJC_85_2024).

#### References

- He Y., Yi W., Suino-Powell K., Zhou X.E., Tolbert W.D., Tang X., Yang J., Yang H., Shi J., Hou L., Jiang H., Melcher K., Xu H.E. Structures and mechanism for the design of highly potent glucocorticoids. *Cell Research* 2014;24:713-26. <https://doi.org/10.1038/cr.2014.52>.
- Zhou M., Qu R., Yin X., Qiu Y., Peng Y., Liu B., Gao Y., Bi H., Guo D. Prednisone acetate modulates Th1/Th2 and Th17/Treg cell homeostasis in experimental autoimmune uveitis via orchestrating the notch signaling pathway. *International Immunopharmacology* 2023;116:109809. <https://doi.org/10.1016/j.intimp.2023.109809>
- Petta I., Peene I., Elewaut D., Vereecke L., De Bosscher K. Risks and benefits of corticosteroids in arthritic diseases in the clinic. *Biochemical Pharmacology* 2019;165:112-25. <https://doi.org/10.1016/j.bcp.2019.04.009>.
- Urquiaga M., Saag K.G. Risk for osteoporosis and fracture with glucocorticoids. *Best Practice & Research: Clinical Rheumatology* 2022;36:101793. <https://doi.org/10.1016/j.berh.2022.101793>.
- Zhang J., Yang Y., Liu W., Schlenk D., Liu J. Glucocorticoid and mineralocorticoid receptors and corticosteroid homeostasis are potential targets for endocrine-disrupting chemicals. *Environment International* 2019;133:105133. <https://doi.org/10.1016/j.envint.2019.105133>.
- Su M., Zhong Y., Xiang J., Chen Y., Liu N., Zhang J. Reproductive endocrine disruption and gonadal intersex induction in male Japanese medaka chronically exposed to betamethasone at environmentally relevant levels. *Journal of Hazardous Materials* 2023;455:131493. <https://doi.org/10.1016/j.jhazmat.2023.131493>.
- Wang C., Li M., Gui W., Shi H., Wang P., Chen J., Fent K., Zhang K., Dai J., Li X., Zhao Y. Prednisolone accelerates embryonic development of zebrafish via glucocorticoid receptor signaling at low concentrations. *Environmental Science & Technology* 2023;57:15794-15805. <https://doi.org/10.1021/acs.est.3c02658>.
- Li M., Wang L., Wang M., Zhao H., Zhao F. Advances on hormones in cosmetics: Illegal addition status, sample preparation, and detection technology. *Molecules* 2023;28:1980. <https://doi.org/10.3390/molecules28041980>.
- Chen D., Chen Y., Zhang Y., Du J., Xiao H., Yang Z., Xu J. Multi-class analysis of 100 drug residues in cosmetics using high-performance liquid chromatography-quadrupole time-of-flight high-resolution mass spectrometry. *Talanta* 2024;266:124954. <https://doi.org/10.1016/j.talanta.2023.124954>.
- Jian L., Yuan X., Han J., Zheng R., Peng X., Wang K. Screening for illegal addition of glucocorticoids in adulterated cosmetic products using ultra-performance liquid chromatography/tandem mass spectrometry with precursor ion scanning. *Rapid Communications in Mass Spectrometry* 2021;35:e8999. <https://doi.org/10.1002/rcm.8999>.
- Kim N.S., Yoo G.J., Lee J.H., Park H.J., Cho S., Shin D.W., Kim Y.L., Beak S.Y. Determination of 43 prohibited glucocorticoids in cosmetic products using a simultaneous LC-MS/MS method. *Analytical Methods* 2017;9:2104-2115. <https://doi.org/10.1039/c6ay03065c>.
- Huang J., Li Y., Xiao S., Fang J. A new glucocorticoid added in cosmetics illegally—Meprednisone. *Flavour Fragr Cosmetics* 2022;4:13-6. <https://doi.org/10.3969/j.issn.1000-4475.2022.04.003>
- Weng D.H., Liu J., Jiang Q.Q., Yang L.P., Zheng L., Xiao D.Q. A new illegal addition of glucocorticoids in cosmetics: Betamethasone butyrate acetate. *Flavour Fragr Cosmetics* 2019;3:45-9. <https://doi.org/10.3969/j.issn.1000-4475.2019.03.011>
- Yang P., Huang W., Li L., Liu H. Determination of new glucocorticoid called clobetasol acetate in cosmetics by ultra performance liquid chromatography-tandem mass spectrometry. *Chinese Journal of Chromatography*. 2023;41:250-6. <https://doi.org/10.3724/sp.j.1123.2022.06010>.
- Nothias L.-F., Petras D., Schmid R., Dührkop K., Rainer J., Sarvepalli A., Protsyuk I., Ernst M., Tsugawa H., Fleischauer M., Aicheler F., Aksenov A.A., Alka O., Allard P.-M., Barsch A., Cachet X., Caraballo-Rodríguez A.M., Da Silva R.R., Dang T., Garg N., Gauglitz J.M., Gurevich A., Isaac G., Jarmusch A.K., Dorrestein P.C. Feature-based molecular networking in the GNPS analysis environment. *Nature Methods* 2020;17:905-8. <https://doi.org/10.1038/s41592-020-0933-6>.
- Marques A.M., Brito L.d.C., Mendonça S.C., Gomes B.A., Camillo F.d.C., Silva G.W.d.S.e., Sampaio A.L.F., Leitão S.G., Figueiredo M.R. An integrated strategy of UHPLC-ESI-MS/MS combined with bioactivity-based molecular networking for identification of antitumoral withanolides from *Athenaea fasciculata* (Vell.) I.M.C Rodrigues & Stehmann. *Molecules* 2024;29:4357. <https://doi.org/10.3390/molecules29184357>.
- Pastuña-Fasso J.V., Quiroz-Moreno C.D., Medina-Villamizar E.J., Cooperstone J.L., Radice M., Peñuela-Mora M.C., Almeida J.R., Mogollón N.G.S. Metabolite fingerprinting of *Urospatha sagittifolia* (Araceae) tubers at different growth stages

- by multi-platform metabolomics and molecular networking. *Microchemical Journal* 2024;199:110058. <https://doi.org/10.1016/j.microc.2024.110058>.
18. Zhu G., Hou C., Yuan W., Wang Z., Zhang J., Jiang L., Karthik L., Li B., Ren B., Lv K., Lu W., Cong Z., Dai H., Hsiang T., Zhang L., Liu X. Molecular networking assisted discovery and biosynthesis elucidation of the antimicrobial spiroketals epicospirocins. *Chemical Communications* 2020;56:10171-10174. <https://doi.org/10.1039/d0cc03990j>.
  19. Wu G., Wang X., Zhang X., Ren H., Wang Y., Yu Q., Wei S., Geng J. Nontarget screening based on molecular networking strategy to identify transformation products of citalopram and sertraline in wastewater. *Water Research* 2023;232:119509. <https://doi.org/10.1016/j.watres.2022.119509>.
  20. Mei S., Yao S., Mo J., Wang Y., Tang J., Li W., Wu T. Integration of cloud-based molecular networking and docking for enhanced umami peptide screening from Pixian Douban. *Food Chemistry: X* 2023;21:101098. <https://doi.org/10.1016/j.fochx.2023.101098>.
  21. Woo I.S., Kim Y.K., Kim H.I., Choi J.D., Han K.M. Characterization of banned colorants in cosmetics: A tandem mass-based molecular networking approach. *Journal of Chromatography A* 2024;1724:464928. <https://doi.org/10.1016/j.chroma.2024.464928>.
  22. Wu X., Xu L.Y., Li E.M., Dong G. Application of molecular dynamics simulation in biomedicine. *Chemical Biology & Drug Design* 2022;99:789-800. <https://doi.org/10.1111/cbdd.14038>.
  23. Singh N., Dalal V., Kumar P. Molecular docking and simulation analysis for elucidation of toxic effects of dicyclohexyl phthalate (DCHP) in glucocorticoid receptor-mediated adipogenesis. *Molecular Simulation* 2020;46:9-21. <https://doi.org/10.1080/08927022.2019.1662002>.
  24. Leng Y., Ren L., Niu S., Zhang T., Zhang J. *In vitro* and *in silico* investigations of endocrine disruption induced by metabolites of plasticizers through glucocorticoid receptor. *Food and Chemical Toxicology* 2021;155:112413. <https://doi.org/10.1016/j.fct.2021.112413>.
  25. Chen Y.C., Wu H.Y., Chang C.W., Liao P.C. Post-deconvolution MS/MS spectra extraction with data-independent acquisition for comprehensive profiling of urinary glucuronide-conjugated metabolome. *Analytical Chemistry* 2022;94:2740-48. <https://doi.org/10.1021/acs.analchem.1c03557>.
  26. Wang X., Li N.\*, Chen S., Ge Y.-H., Xiao Y., Zhao M., Wu J.-L. MS-FINDER assisted in understanding the profile of flavonoids in temporal dimension during the fermentation of pu-erh tea. *Journal of Agricultural and Food Chemistry* 2022;70:7085-7094. <https://doi.org/10.1021/acs.jafc.2c01595>.
  27. Zeng J., Li Y., Wang C., Fu S., He M. Combination of *in silico* prediction and convolutional neural network framework for targeted screening of metabolites from LC-HRMS fingerprints: A case study of "Pericarpium citri reticulatae - Fructus aurantii". *Talanta* 2024;269:125514. <https://doi.org/10.1016/j.talanta.2023.125514>.
  28. Schymanski E.L., Jeon J., Gulde R., Fenner K., Ruff M., Singer H.P., Hollender J. Identifying small molecules via high resolution mass spectrometry: Communicating confidence. *Environmental Science & Technology* 2014;48:2097-8. <https://doi.org/10.1021/es5002105>.
  29. Tunyasuvunakool K., Adler J., Wu Z., Green T., Zielinski M., Židek A., Bridgland A., Cowie A., Meyer C., Laydon A., Velankar S., Kleywegt G.J., Bateman A., Evans R., Pritzel A., Figurnov M., Ronneberger O., Bates R., Kohl S.A.A., Potapenko A., Ballard A.J., Romera-Paredes B., Nikolov S., Jain R., Clancy E., Reiman D., Petersen S., Senior A.W., Kavukcuoglu K., Birney E., Kohli P., Jumper J., Hassabis D. Highly accurate protein structure prediction for the human proteome. *Nature* 2021;596:590-6. <https://doi.org/10.1038/s41586-021-03828-1>.
  30. Maloney F.P., Kuklewicz J., Corey R.A., Bi Y., Ho R., Mateusiak L., Pardon E., Steyaert J., Stansfeld P.J., Zimmer J. Structure, substrate recognition and initiation of hyaluronan synthase. *Nature* 2022;604:195-201. <https://doi.org/10.1038/s41586-022-04534-2>.
  31. Chen S.Y., Fang M., Lin Y.T., Tsai C.F., Cheng H.F., Wang D.Y. Elucidation of two new corticosteroids, betamethasone dibutyrate and betamethasone tributryrate. *Steroids* 2021;165:108739. <https://doi.org/10.1016/j.steroids.2020.108739>.
  32. Khader Kal A.K., Karatt T.K., Nalalath J., Subhakar M.B., Koshy S.A., Perwad Z., Ajeesbanu M.P. Simultaneous analysis of 44 frequently abused corticosteroid drugs using polysaccharide-based chiral column-HRMS approach. *Analytical Science Advances* 2021;2:427-439. <https://doi.org/10.1002/ansa.202000166>.
  33. Karatt T.K., Nalalath J., Perwad Z., Albert P.H., Khader K.K.A., Padusha M.S.A., Laya S. Mass spectrometric method for distinguishing isomers of dexamethasone via fragment mass ratio: An HRMS approach. *Journal of Mass Spectrometry: JMS* 2018;53:1046-1058. <https://doi.org/10.1002/jms.4279>.
  34. Yang W., Yang X., Shi F., Liao Z., Liang Y., Yu L., Wang R., Li Q., Bi K. Qualitative and quantitative assessment of related substances in the compound ketoconazole and clobetasol propionate cream by HPLC-TOF-MS and HPLC. *Journal of Pharmaceutical Analysis* 2019;9:156-162. <https://doi.org/10.1016/j.jpba.2018.08.006>.
  35. Salem I.I., Alkhatib M., Najib N. LC-MS/MS determination of betamethasone and its phosphate and acetate esters in human plasma after sample stabilization. *Journal of Pharmaceutical and Biomedical Analysis* 2011;56:983-991. <https://doi.org/10.1016/j.jpba.2011.07.020>.
  36. Lee J.-H., An T.-G., Kim S.J., Shim W.-S., Lee K.-T. Development of liquid chromatography tandem mass spectrometry method for determination of spironolactone in human plasma: Application to a bioequivalence study of Daewon Spiracton Tablet® (spironolactone 50 mg). *Journal of Pharmaceutical Investigation* 2015;45:601-9. <https://doi.org/10.1007/s40005-015-0197-9>.
  37. Sparidans R.W., van Velsen S.G., de Roos M.P., Schellens J.H., Bruijnzeel-Koomen C.A., Beijnen J.H. Liquid chromatography-tandem mass spectrometric assay for clobetasol propionate in human serum from patients with atopic dermatitis. *Journal of Chromatography B* 2010;878:2150-4. <https://doi.org/10.1016/j.jchromb.2010.06.011>.
  38. Guo C., Gong L., Wang W., Leng J., Zhou L., Xing S., Zhao Y., Xian R., Zhang X., Shi F. Rapid screening and identification of targeted or non-targeted antitussive adulterants in herbal medicines by q-orbitrap HRMS and screening database. *International Journal of Mass Spectrometry* 2020;447:116250. <https://doi.org/10.1016/j.ijms.2019.116250>.
  39. Sasse M., Rainer M. Mass spectrometric methods for non-targeted screening of metabolites: A future perspective for the identification of unknown compounds in plant extracts. *Separations* 2022;9:415. <https://doi.org/10.3390/separations9120415>.
  40. Giaccone V., Polizzotto G., Macaluso A., Cammilleri G., Ferrantelli V. Determination of ten corticosteroids in illegal cosmetic products by a simple, rapid, and high-performance LC-MS/MS method. *International Journal of Analytical Chemistry* 2017;2017:3531649. <https://doi.org/10.1155/2017/3531649>.
  41. Meng X., Bai H., Guo T., Niu Z., Ma Q. Broad screening of illicit ingredients in cosmetics using ultra-high-performance liquid chromatography-hybrid quadrupole-orbitrap mass spectrometry with customized accurate-mass database and mass spectral library. *Journal of Chromatography A* 2017;1528:61-74. <https://doi.org/10.1016/j.chroma.2017.11.004>.
  42. National Medical Products Administration. Determination of hormone components in cosmetics. NO.66, Annex 1, 2019-09-17. Available from: <https://www.nmpa.gov.cn/hzhp/hzhpfgwj/hzhpzgwj/20190927152001264.html>. Accessed March 22, 2025.
  43. Faiyazuddin M., Ahmad N., Khar R.K., Bhatnagar A., Ahmad F.J. Stabilized terbutaline submicron drug aerosol for deep lungs deposition: Drug assay, pulmonokinetics and biodistribution by UHPLC/ESI-Q-TOF-MS method. *International Journal of Pharmaceutics* 2012;434:59-69. <https://doi.org/10.1016/j.ijpharm.2012.05.007>.
  44. Noh E., Yoon C.-Y., Lee J.H., Lee J.-m., Baek S.-Y., Oh H.B., Do J.-A. A liquid chromatography-quadrupole-time of flight mass spectrometry (LC-Q-TOF MS) study for analyzing 35 corticosteroid compounds: Elucidation of MS/MS fragmentation pathways. *Bulletin of the Korean Chemical Society* 2016;37:1029-1038. <https://doi.org/10.1002/bkcs.10814>.
  45. Sophia A., Faiyazuddin M., Alam P., Hussain M.T., Shakeel F. GC-MS characterization and evaluation of antimicrobial, anticancer and wound healing efficiency of combined ethanolic extract of *Tridax procumbens* and *Acalypha indica*. *Journal of Molecular Structure* 2022;1250:131678. <https://doi.org/10.1016/j.molstruc.2021.131678>.
  46. Li K., Gao Y., Li X., Zhang Y., Zhu B., Zhang Q. Fragmentation pathway of organophosphorus flame retardants by liquid chromatography-orbitrap-based high-resolution mass spectrometry. *Molecules (Basel, Switzerland)* 2024;29:680. <https://doi.org/10.3390/molecules29030680>.
  47. Shlivko I.L., Kamensky V.A., Donchenko E.V., Agrba P. Morphological changes in skin of different phototypes under the action of topical corticosteroid therapy and tacrolimus. *Skin Research and Technology* 2014;20:136-140. <https://doi.org/10.1111/srt.12095>.
  48. Niculet E., Bobeica C., Tatu A.L. Glucocorticoid-induced skin atrophy: The old and the new. *Clinical, Cosmetic and Investigational Dermatology* 2020;13:1041-1050. <https://doi.org/10.2147/CCID.S224211>.
  49. Norsgaard H., Kurdykowski S., Descargues P., Gonzalez T., Marstrand T., Dünstl G., Røpke M. Calcipotriol counteracts betamethasone-induced decrease in extracellular matrix components related to skin atrophy. *Archives of Dermatological Research* 2014;306:719-29. <https://doi.org/10.1007/s00403-014-1485-3>.
  50. Tan H., Chen Q., Hong H., Benfenati E., Gini G.C., Zhang X., Yu H., Shi W. Structures of endocrine-disrupting chemicals correlate with the activation of 12 classic nuclear receptors. *Environmental Science and Technology* 2021;55:16552-16562. <https://doi.org/10.1021/acs.est.1c04997>.
  51. Liang Y., Li Z., Zhang J., Li T., Lv C. Comparison of the glucocorticoid receptor binding and agonist activities of typical glucocorticoids: Insights into their endocrine disrupting effects. *Chemistry & Biodiversity* 2024;21:e202301525. <https://doi.org/10.1002/cbdv.202301525>.
  52. Zou H., Yu J., Li Z., Liu Y., Wang T., Li T., Lv C., Zhang J. *In vitro*, *in vivo*, and *in silico* evaluation of the glucocorticoid receptor antagonist activity of 3,6-dibromocarbazole. *Food and Chemical Toxicology* 2023;180:114048. <https://doi.org/10.1016/j.fct.2023.114048>.
  53. Guo D., Liu Y., Liang J., Huang Y., Li Y., Fang J., Yin S. Non-targeted screening and toxicity study of safety risk substances in facial skincare products: Molecular networking and computational toxicology strategy. *Journal of Dermatologic Science and Cosmetic Technology* 2024;1:100055. <https://doi.org/10.1016/j.jdsct.2024.100055>.